

RESEARCH ARTICLE SUMMARY

NEUROEVOLUTION

Molecular diversity and evolution of neuron types in the amniote brain

David Hain^{†*}, Tatiana Gallego-Flores^{†*}, Michaela Klinkmann, Angeles Macias, Elena Ciurdaeva, Anja Arends, Christina Thum, Georgi Tushev, Friedrich Kretschmer, Maria Antonietta Tosches^{†‡}, Gilles Laurent^{†*}

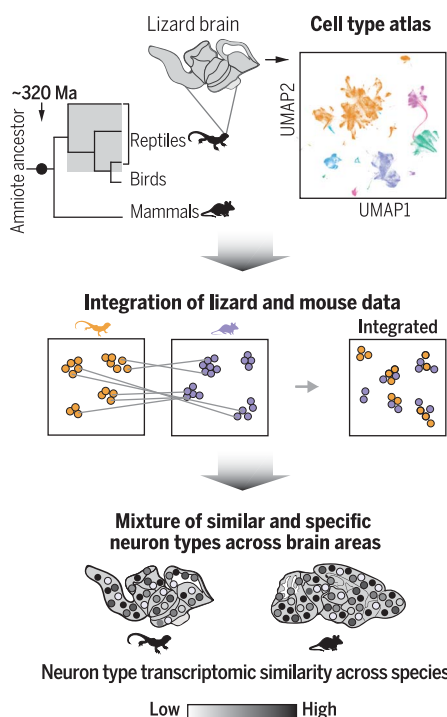
INTRODUCTION: Vertebrate evolution took an important turn before the onset of the Permian, 320 million years ago, with the transition of early tetrapods from water to land, the appearance of amniotes, and, soon thereafter, their bifurcation into sauropsids (future reptiles and birds) and synapsids (future mammals). Despite this branched history, the brains of all tetrapods share the same ancestral architecture defined by brain regions established during embryonic development (pallium, subpallium, thalamus, cerebellum, etc.) and by their long-range connections. Yet how variations on this common organization contributed to lineage- and species-specific adaptations is not clear. A commonly held assumption, for example, is that subcortical regions are ancient and “deeply conserved,” whereas the mammalian cortex is “new,” following profound changes in cortical development in this lineage.

Brain regions, however, do not operate in isolation, raising the possibility that the evolution of interconnected neurons might be correlated. Likewise, areas in reptiles and mammals that derive from a common ancestral structure, such as the cerebral cortex, may have evolved in each lineage in such a way that they now each contain both ancient (thus common) and novel neuron types. Because traditional comparisons of developmental regions and projections may not suffice to reveal these similarities and differences, we investigated these issues using cellular transcriptomic approaches.

RATIONALE: Neurons are the most diverse cell types in the brain; their evolutionary diversification reflects changes in the developmental processes that produce them and, in turn, may drive changes in the neural circuits to which they belong. To the extent that a neuron’s transcriptome represents the molecular encoding of its identity, connectivity, and developmental and evolutionary histories, comparing neuronal transcriptomes across species should yield insights into brain evolution. To elucidate the evolution of neuronal diversity across brain regions, we generated a cell type atlas of the brain of a reptile, the Australian bearded

dragon *Pogona vitticeps*, and compared it with existing mouse brain datasets.

RESULTS: We profiled 285,483 single-cell transcriptomes from the brain of *Pogona* and identified and annotated 233 distinct types of neurons. Computational integration of this dataset with publicly available mouse data revealed that lizard and mouse neurons co-cluster according to their regional and neurotransmitter identities. These integrated clusters expressed distinctive combinations of de-



Transcriptomic study of neuronal evolution

among amniotes. Reptiles and mammals evolved independently of each other for ~300 million years. We generated a cell type atlas from the brain of a lizard, *Pogona vitticeps*. Computational integration of these data with mouse transcriptomes reveals that telencephalon, diencephalon, and mesencephalon each contain mixtures of similar and divergent neurons, indicating that neuron diversification is ubiquitous in those regions.

velopmental transcription factors (including homeodomain-type) and genes involved in neuronal connectivity (cell junction, synaptic signaling, neuronal projections, synaptic transmission), indicating that both developmental origin and circuit allocation define broad, evolutionarily conserved classes of neurons in the amniote brain.

At a finer level, these broad classes included neuron types with a wide range of transcriptomic variation across species. Certain neuron types could be readily mapped from lizard to mouse, indicating high transcriptomic similarity; others, however, could not be mapped across species unambiguously, owing to transcriptomic divergence. This dichotomy was true for all regions analyzed (telencephalon, diencephalon, and midbrain), indicating that neuronal diversification is ubiquitous in these brain regions.

This was particularly evident in the thalamus, where neurons with high transcriptomic similarity across species (GABAergic reticular thalamic nucleus, glutamatergic “medial thalamus”) are juxtaposed with neuron types with diverging gene expression (glutamatergic “lateral thalamus”). In the lateral thalamus, lizard and mouse neurons from sensory relay nuclei did not co-cluster according to sensory modality, suggesting that these neurons may have diversified extensively, reflecting the different fates of their cortical partners in the reptilian and mammalian lineages.

CONCLUSION: Using comparative single-cell transcriptomics, we identified a core set of neuron types with high transcriptomic similarity between the brains of a lizard and a mammal, despite 320 million years of separate evolution. These neuron types are not restricted to subcortical regions but are found everywhere in the brain, including in the cerebral cortex, challenging the notion that certain brain regions are more ancient than others. Our data suggest that, even if the brain consists of developmental modules defined by ancient and shared molecular determinants, the evolution of the brain acts upon each module by keeping (e.g., reticular thalamic nucleus and medial thalamus) or diversifying (e.g., lateral thalamus) neuron types in a manner that is correlated with local and long-range connectivity. ■

The list of author affiliations is available in the full article online.

*Corresponding author. Email: david.hain@brain.mpg.de (D.H.); maria-tatiana.gallego-flores@brain.mpg.de (T.G.-F.); mt335@columbia.edu (M.A.T.); gilles.laurent@brain.mpg.de (G.L.)

†These authors contributed equally to this work.

‡These authors contributed equally to this work.

Cite this article as D. Hain et al., *Science* **377**, eabp8202 (2022). DOI: 10.1126/science.abp8202

S READ THE FULL ARTICLE AT
<https://doi.org/10.1126/science.abp8202>

RESEARCH ARTICLE

NEUROEVOLUTION

Molecular diversity and evolution of neuron types in the amniote brain

David Hain^{1,2†*}, Tatiana Gallego-Flores^{1,2†*}, Michaela Klinkmann¹, Angeles Macias¹, Elena Ciardaeva¹, Anja Arends¹, Christina Thum¹, Georgi Tushev¹, Friedrich Kretschmer¹, Maria Antonietta Tosches^{1,3‡*}, Gilles Laurent^{1‡*}

The existence of evolutionarily conserved regions in the vertebrate brain is well established. The rules and constraints underlying the evolution of neuron types, however, remain poorly understood. To compare neuron types across brain regions and species, we generated a cell type atlas of the brain of a bearded dragon and compared it with mouse datasets. Conserved classes of neurons could be identified from the expression of hundreds of genes, including homeodomain-type transcription factors and genes involved in connectivity. Within these classes, however, there are both conserved and divergent neuron types, precluding a simple categorization of the brain into ancestral and novel areas. In the thalamus, neuronal diversification correlates with the evolution of the cortex, suggesting that developmental origin and circuit allocation are drivers of neuronal identity and evolution.

Vertebrates arose during the Cambrian explosion, about half a billion years ago. Despite this long history, their brains share a common basic architecture, including the same identifiable brain divisions: forebrain (telencephalon and diencephalon), midbrain or mesencephalon, and hindbrain or rhombencephalon (metencephalon and myelencephalon). This stability of brain architecture can be contrasted with that in other animal clades, such as mollusks, who, over the same period, evolved a greater variety of nervous system plans and neural circuits (1).

During early vertebrate development, the principal brain divisions are patterned by conserved signaling centers and express similar combinations of developmental transcription factors (2–4). Those divisions develop into brain regions (e.g., pallium, basal ganglia, thalamus, optic tectum, etc.) containing increasingly clade-specific circuits and neuron types. For example, both mammals and nonavian reptiles have a layered cerebral cortex and a thalamus, although with different numbers of cortical layers and thalamic nuclei (5).

Two extreme models could explain the evolution of neuronal diversity in the brain. If neuronal identity were strongly tied to developmental history, then neurons that belong to the same brain region would be expected to evolve in concert and to display similar rates

of molecular divergence from their respective orthologs in other species (Fig. 1A, model 1). By contrast, if the genetic programs that specify brain regions and neuronal identities were, at least in part, independent of one another, then neurons in the same brain region would be free to evolve along distinct paths at different rates. In this case, each brain region would be a mosaic of conserved (i.e., shared across species) and diverging (i.e., specific) neuron types (Fig. 1A, model 2).

To test these models, we quantified and systematically compared neuronal diversity in two amniotes, the mouse and a lizard, the Australian bearded dragon *Pogona vitticeps*, using cellular transcriptomes as proxies for neuronal identities. The common ancestor of mammals and reptiles lived some 320 million years ago, had already fully adapted to life on land, and had a complex brain with a cerebral cortex (6).

Our analysis indicates that brain regional identities are encoded in neuronal transcriptomes by conserved sets of genes, that a core set of deeply conserved neuron classes can be identified in the two species, and that neuronal diversification has occurred in mammals and in reptiles in all the brain divisions that we analyzed in detail (telencephalon, diencephalon, and mesencephalon). This changes and clarifies, at a cellular scale, the simple perspective that certain regions of the vertebrate brain are ancient, while others are new. We propose that most brain regions, in reptiles as in mammals, contain a mixture of ancient and novel neuron types. Within this scheme, we observe interesting local variations, such as across the medial and lateral domains of the thalamus, that parallel the divergent evolution of the cerebral cortex in reptiles and mammals.

A cell type atlas of the lizard brain

To build a cell type atlas of the adult *Pogona* brain, we performed single-cell RNA sequencing (scRNA-seq; 10X Chromium) on 285,483 cells sampled from the telencephalon, diencephalon, mesencephalon, and metencephalon (with the exception of the olfactory bulb and pineal complex, and with a limited sampling of the noncerebellar metencephalon) (figs. S1, S2A, and S3A) (see methods in the supplementary materials). Clustering analysis identified classes of neuronal and non-neuronal cells (Fig. 1B) annotated for the expression of canonical marker genes (Fig. 1C and fig. S2B). For example, neurons were identified by expression of *snap25*, part of the SNARE (soluble *N*-ethylmaleimide-sensitive factor attachment protein receptor) machinery (7); oligodendrocyte precursor cells (OPCs) by *pdgfra*, a receptor for platelet-derived growth factor (8); differentiating oligodendrocytes by *gpr17* (9) and *mag* (10); mature oligodendrocytes by *mag* but not *gpr17*; ependymoglia cells by *gfap* (11), suggestive of a common origin with mammalian astrocytes (12); a population of ependymoglia in the cerebellum (a putative reptilian homolog of Bergmann glia) by *draxin*, an axon guidance molecule (13); and cells from the subcommissural organ by *sspo*, involved in the formation of the Reissner's fiber (14).

We focused on the 89,015 neurons in our data, revealing 233 distinct clusters (Fig. 1D and fig. S3C). We assigned each cluster to one of 11 brain regions (Fig. 1D) using several criteria: (i) knowledge of origin by dissection before dissociation (figs. S3, A to C, and S4, and data S1); (ii) expression patterns of cluster-specific marker genes, assayed by in situ hybridization; and (iii) expression of known region-specific marker genes described in the literature (data S2 and S3).

An analysis of the expression of gene families across lizard neuron types indicated that, as reported in other systems (15–17), certain gene families, such as G protein-coupled receptors (GPCRs) and transcription factors (especially of the homeodomain type), show cell type-specific expression (Fig. 1E). This supports the hypothesis that homeodomain transcription factors function as selectors of neuronal identity in both vertebrates and invertebrates (17). Because transcription factors, including homeodomain types, are crucial for the early regionalization of the vertebrate nervous system, we sought to determine whether the expression of transcription factors in adult neuron types is sufficient to group them according to the brain regions to which they belong. For this, we performed hierarchical clustering of cluster transcriptomes on the basis of the expression of the 386 transcription factors expressed in the dataset.

The resulting taxonomy grouped neuronal clusters not only by brain region but also by

¹Max Planck Institute for Brain Research, Frankfurt am Main, Germany. ²Faculty of Biological Sciences, Goethe University, Frankfurt am Main, Germany. ³Department of Biological Sciences, Columbia University, New York, NY, USA.

*Corresponding author. Email: david.hain@brain.mpg.de (D.H.); maria-tatiana.gallego-flores@brain.mpg.de (T.G.-F.); mt3353@columbia.edu (M.A.T.); gilles.laurent@brain.mpg.de (G.L.).

†These authors contributed equally to this work.

‡These authors contributed equally to this work.

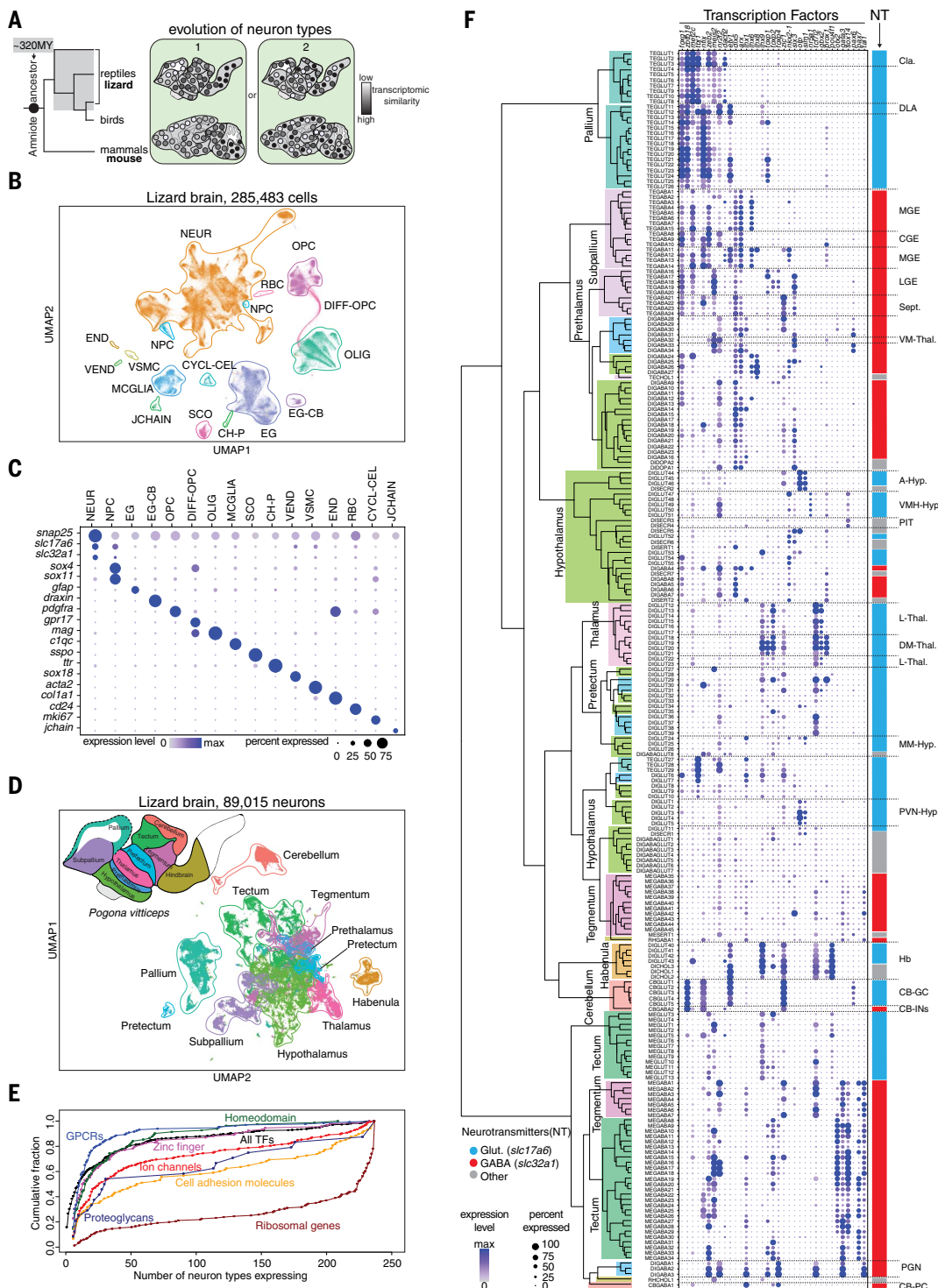


Fig. 1. Large-scale scRNA-seq on *Pogona* brain reveals 233 neuron clusters.

(A) (Left) Schematic of the phylogenetic position of mammals and reptiles. MY, million years ago. (Right) Two possible models of the evolution of neuronal types in the brain (lizard brain, top; mouse brain, bottom). **(B)** Uniform manifold approximation and projection (UMAP) representation of 285,483 single-cell transcriptomes from the brain of *Pogona*. Cells are color coded by cluster. NEUR, neurons; OPC, oligodendrocyte progenitor cells; DIFF-OPC, differentiating oligodendrocyte progenitor cells; OLIG, oligodendrocytes; EG, ependymoglia; EG-CB, ependymoglia cerebellum; CH-P, choroid plexus; SCO, subcommissural organ; CYCL-CEL, cycling cells; MCGLIA, microglia; VEND, vascular endothelial

cells; VSMC, vascular smooth muscle cells; JCHAIN, plasma cells; END, endothelial cells; NPC, neural progenitor cells; RBC, red blood cells.

(C) Expression of cell type–specific marker genes across clusters. Dot diameter represents fraction of cells in which the gene is detected; color represents expression level. **(D)** UMAP embedding of 89,015 single-neuron transcriptomes colored by assigned brain region. **(E)** Cumulative distribution plot of number of neuron types expressing genes in the following families: homeodomain transcription factors (TFs), zinc finger TFs, all TF families, GPCRs, ion channels, proteoglycans, cell adhesion molecules, and ribosomal genes. Each dot is a gene. **(F)** Dendrogram of 233 neuronal clusters based on average transcription

factor expression (only 35 of 386 TFs are shown). Colors indicate brain regions (left) and neurotransmitters (right); glutamate, blue: *slc17a6*; GABA, red: *slc32a1*; other, gray: *slc17a6* and *slc32a1*; *chat* and *slc18a3*; *th*, *ddc*, and *slc18a2*; or *tph1/tph2* and *slc18a2*. Cla., claustrum; DLA, dorsolateral amygdala; MGE, medial ganglionic eminence; CGE, caudal ganglionic eminence; LGE, lateral ganglionic eminence; Sept., Septum; VM-Thal., ventromedial thalamic

nucleus; A-Hyp., anterior hypothalamus; VMH-Hyp., ventromedial hypothalamus; PIT, pituitary gland; L-Thal., lateral thalamic nucleus; DM-Thal., dorsomedial thalamic nucleus; MM-Hyp., mammillary hypothalamus; PVN-Hyp., paraventricular hypothalamus; Hb, habenula; CB-GC, cerebellar granule cells; CB-INs, cerebellar interneurons; PGN, pretectal geniculate nucleus; CB-PC, cerebellar Purkinje cells.

neurotransmitter type (Fig. 1F). Brain regions and individual nuclei within them (spatially validated by the criteria listed above) are thus identifiable by the combinatorial expression of sets of transcription factors. For example, telencephalic glutamatergic neurons could be distinguished by the coexpression of *foxg1* and *zbtb18* (18); thalamic glutamatergic neurons by *tcf7l2* and *lhx9* (19, 20); habenular neurons by *tcf7l2*, *zic1*, *lhx9*, and *pou4f1* (19); cerebellar granule cells and interneurons, but not Purkinje cells, by *zic1*, *zbtb18*, and *nfia* (21); medial ganglionic eminence-derived γ -aminobutyric acid-releasing (GABAergic) neurons by *foxg1*, *arx*, *lhx6*, *dlx5*, and *zeb2* (22); lateral ganglionic eminence-derived GABAergic neurons by *foxg1*, *meis2*, and *dlx5* (23); and GABAergic neurons of the tegmentum and tectum express *tal1* and *gata3*, but mostly tegmental neurons express *nr2f2* (24) (Fig. 1F). Using *in situ* hybridization and data available in the literature (data S2), we identified individual nuclei within these brain regions, such as the claustrum and dorsolateral amygdala in the pallium (25); septum in the subpallium; dorsomedial thalamic nucleus in the thalamus; and paraventricular, ventromedial, and mammillary nuclei in the hypothalamus (Fig. 1F and data S2). All 233 clusters and the expression of some of the transcription factors used for their annotation are shown in Fig. 1F and fig. S3C.

Transcriptomic comparisons reveal shared classes of neuron types

Many region- and neuron type-specific marker genes identified in *Pogona* (Fig. 1F and fig. S3C) corresponded to those described in mammals (3). To examine in detail interspecies similarities and differences of neuron types, we integrated our lizard data with a published mouse brain dataset of comparable size and complexity [70,968 neurons, 181 clusters (26)] (fig. S5A). We used canonical correlation analysis (CCA) (27) to identify vectors of genes with high variance across both datasets and then used the 40 top canonical components for downstream analysis, including clustering on the joint nearest-neighbors graph (“integrated clusters”). Twenty of the 32 integrated clusters obtained (Fig. 2A) included neurons of both species (defined as >10% of neurons from each of the two species), indicating that our analysis captures molecular signatures shared across species. Among the integrated clusters with <10% of lizard neurons, some corresponded to mouse neuron types with no lizard homolog [for in-

stance, mouse neocortical layer 6 neurons, cluster 19 (12)], while others (such as cluster 18, olfactory bulb) were neuron types not included in our lizard tissue selections (Fig. 2A and figs. S3A, S5, and S6A). Most neurons in each integrated cluster originated from the same brain divisions (telencephalon, diencephalon, mesencephalon, and metencephalon) in both species (Fig. 2A and fig. S6A), suggesting that the integrated clusters share molecular signatures that reflect their regional identity. Because the main divisions of the developing brain are evolutionarily conserved among vertebrates (28), we hypothesize that these integrated clusters are evolutionarily conserved classes of neuron types. Integrated clusters include, for example, GABAergic neurons from the lateral (cluster 11), medial (cluster 16), and caudal (cluster 17) ganglionic eminences; habenular neurons (cluster 23); cerebellar inhibitory neurons (cluster 24) and granule cells (cluster 9); and glutamatergic and GABAergic cells from the lizard optic tectum and mouse superior colliculus (clusters 2 and 13, respectively) (Fig. 2A and fig. S6A).

To identify the gene families that underlie the co-clustering of mouse and lizard single neurons, we identified marker genes specific to the integrated clusters and present in neurons of both species (data S4). A gene ontology analysis of these marker genes revealed an enrichment in transcription factors, genes related to neuronal connectivity (cell junction, synaptic signaling, neuronal projections, synaptic transmission) and to neuronal development (fig. S6B). Among the conserved transcription factors, the most represented group belonged to the homeodomain type (fig. S6C; homeodomain-type transcription factors are also the largest category among the one-to-one orthologous transcription factors). To check that transcription factors are expressed in evolutionarily conserved patterns, we performed *in situ* hybridization with representatives of different transcription factor families, such as *tcf7l2*, member of the high-mobility group (HMG) box (thalamus and habenula); *mef2c*, a myocyte-specific enhancer-binding factor 2 gene (pallium and medial and lateral ganglionic eminences); *zic1*, a C2H2 zinc finger protein gene (septum, cerebellar granule cells, and anterior prethalamus and medial thalamus); or *tbr1*, a T-box brain transcription factor (pallium) (Fig. 2B). Taken together, these results indicate that sets of transcription factors and effector genes

common to the lizard and mouse brains can be used to identify not only conserved gene expression territories (3) but, more specifically, classes of neuron types common to both species.

Brain regions include similar and divergent neuron types

Taxonomies are often hierarchical. In a comparative context, it has been observed in mammals that higher levels of a cell type taxonomy (e.g., class and subclass) are more conserved than lower ones (e.g., type and subtype) (29). The integration of mouse and lizard single-cell transcriptomes identified large classes of neurons with high cross-species similarity but proved insufficient to identify similarities at the level of individual neuron types (Fig. 2). We reasoned that, if highly similar lizard and mouse neuron types or subtypes existed, they would be “hidden” within the classes of neurons identified above. To identify similarities at deeper levels of the taxonomy, we used the 181 mouse clusters as references and projected the 89,015 lizard single-neuron transcriptomes onto them (26) on the basis of their distances in their joint-embedding space (Fig. 3A; details in methods). The numbers of neurons in each lizard cluster that projected onto a mouse cluster were used to define “projection scores” (normalized; see methods), reflecting the transcriptomic similarity of cluster pairs across species. One hundred and fifty four of the 181 mouse clusters (26) had lizard cells projecting onto them (Fig. 3A). Projection scores ranged widely (fig. S7, A and B), indicating that neuron types or subtypes can diverge widely at the molecular level, even when they belong to evolutionarily conserved classes of neurons. Many of the neuron types with the highest projection scores (0.4 or above) between lizards and mice were those for which homologies had been suggested on the basis of neuroanatomy and expression of selected marker genes. They include neurons in the claustrum and habenula, striatal medium spiny neurons, cerebellar granule cells, interneurons, and Purkinje cells (Fig. 3A) (25, 30–32). We also discovered previously unknown putatively conserved neuron types, such as certain cortical GABAergic interneurons (e.g., coexpressing *sst*, *nos1*, and *chodl*), glutamatergic neurons in the medial thalamus, and neurons from the mouse reticular thalamic nucleus (Fig. 3A). Neuron types that are thought to have evolved similar transcriptomes by convergence (in the reptilian anterior dorsal ventricular ridge and layer 4 of the mammalian

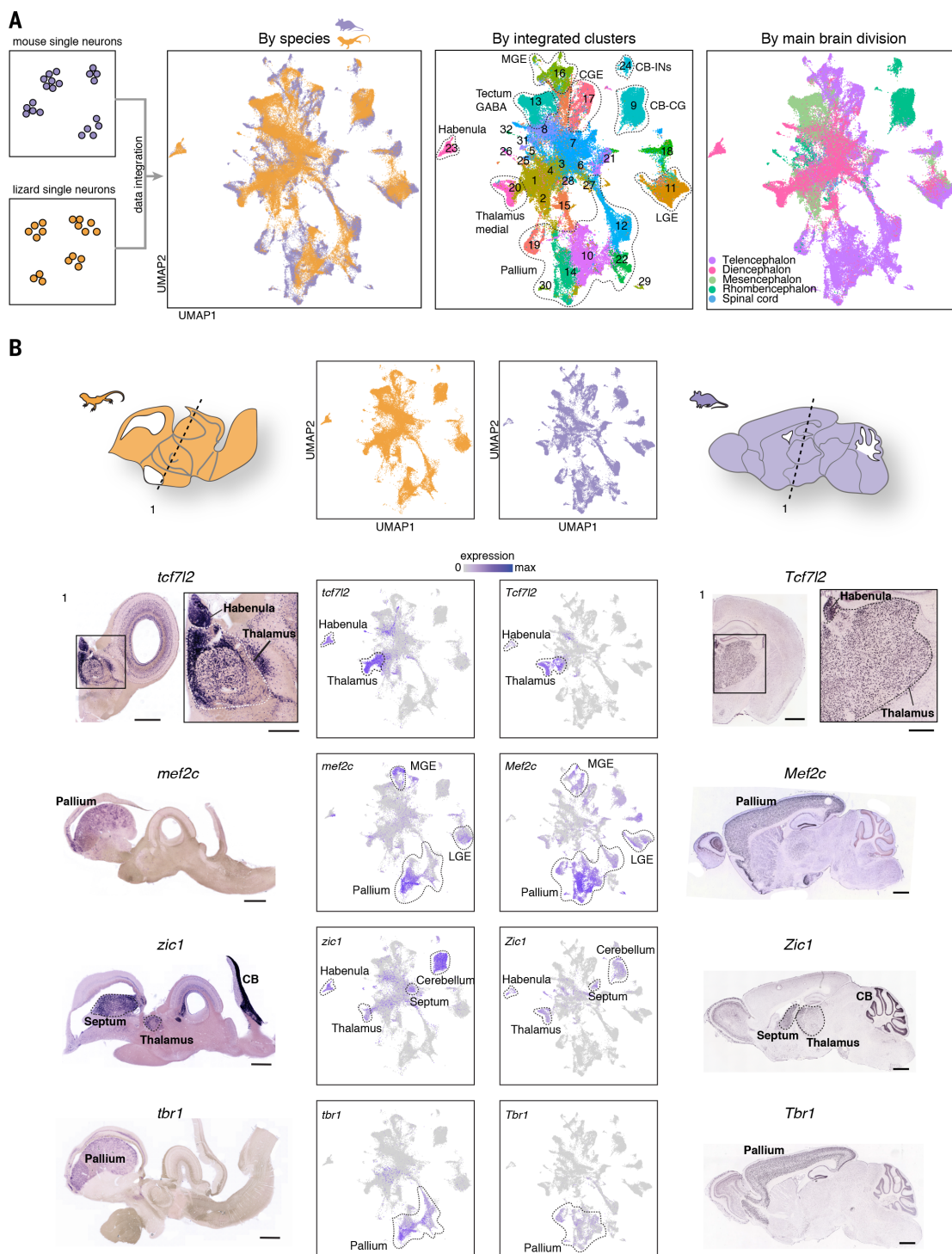


Fig. 2. Comparative analysis of *Pogona* and mouse single-neuron transcriptomes reveals 20 shared neuron-type families. (A) Schematic of CCA-based integration and the UMAP representation of 123,638 integrated single-cell transcriptomes from mouse and *Pogona*. Cells colored by species of origin (left), integrated clusters (1 to 32, middle), and brain division (right). (B) Coronal (top) and sagittal (bottom three) sections of *Pogona* (leftmost column) and mouse

(rightmost column) brain stained by *in situ* hybridization for the following genes: *tcf7l2*, *mef2c*, *zic1*, and *tbr1*. UMAPs (integrated coordinates, middle two columns) showing the expression of the same genes for cells from *Pogona* (left) and mouse (right). Mouse sections from Allen Mouse Brain Atlas (66). Location of transverse section (labeled “1”) indicated in schematic at top. Scale bars: 1 mm (main images) and 500 μ m (insets).

neocortex) (12) also showed high projection scores. We confirmed the localization of some of these neuron types by *in situ* hybridization [Fig. 3C and fig. S8A; *foxp2* for medial and

dorsal habenula; *gbx2* for medial thalamus (mouse: paraventricular thalamus; lizard: dorsomedial thalamus); *meis2* for prethalamus (mouse: reticular thalamic nucleus; lizard: ventromedial

thalamic nucleus), and *gng13* for cerebellar Purkinje cells].

To assess whether the numbers of transcriptomically similar neuron types differed

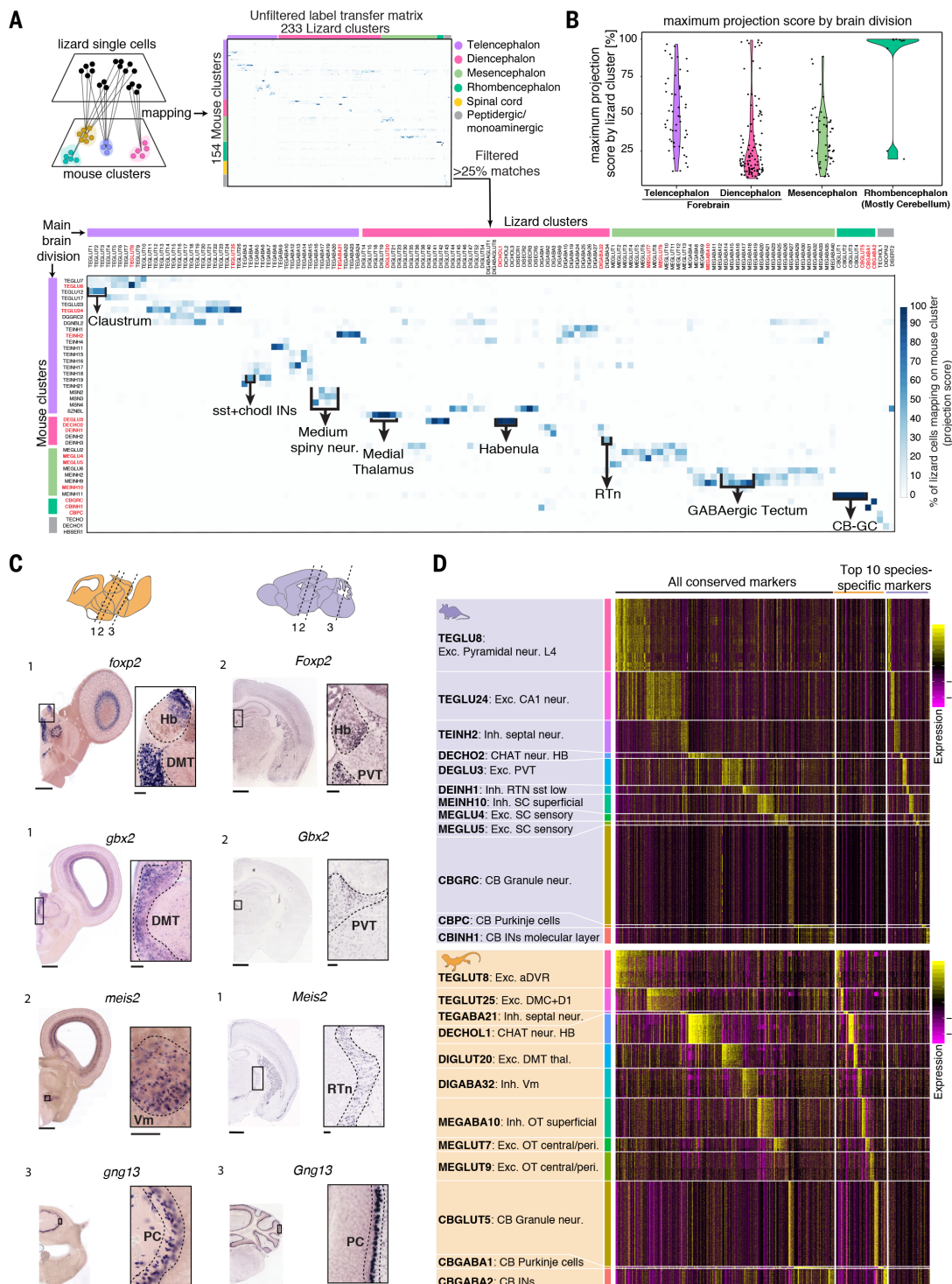


Fig. 3. Comparative analysis reveals a mix of conserved and divergent neuron types in most areas of the forebrain and midbrain. (A) Schematic of label transfer-based integration of lizard and mouse clusters (top left). Unfiltered (top right) and filtered (bottom) matrix (filter for >25% matches of transcriptomic similarity between *Pogona* and mouse clusters). Look-up table: fraction of *Pogona* single-cell transcriptomes from a cluster mapping to a specific mouse cluster (see methods). Selected cluster pairs are shown in red (matrix row and column labels). (B) Maximum projection score for each lizard cluster by brain region. Each dot represents the highest projection score for a lizard

cluster. Note that rhombencephalon samples were mostly from the cerebellum. (C) Coronal sections from adult *Pogona* (left) and mouse (right) brains with *in situ* staining for *foxp2*, *Gbx2*, *meis2*, and *gng13*. Schematic (top) shows approximate section position. Mouse sections from Allen Mouse Brain Atlas (66). Scale bars: 1 mm (main images) and 200 μ m (insets). PVT, paraventricular thalamus; DMT, dorsomedial thalamus; RTn, reticular thalamic nucleus; Vm, ventromedial thalamic nucleus; PC, Purkinje cells. (D) Expression of conserved and top 10 species-specific marker genes for *Pogona* (orange) and mouse (purple) selected cluster pairs. Mouse clusters, top; lizard clusters, bottom.

significantly between main brain divisions (telencephalon, diencephalon, mesencephalon, and metencephalon), we plotted the highest projection score per lizard cluster for each such division (Fig. 3B). These scores were widely distributed within individual divisions. Indeed, all main brain divisions (except for the cerebellum), contained both high and low scores, suggesting that they contain both molecularly similar and divergent cell types (Fig. 3B).

We chose three cell type pairs with high projection scores for each brain division from lizard and mouse and examined the similarities and differences in gene expression between them (Fig. 3D). For each one of these highly similar pairs of neuron types, we identified both common marker genes and mouse- or lizard-specific markers (Fig. 3D and data S5, S6, and S7). Finally, we validated our comparisons of mouse and lizard single-cell transcriptomes—based on Seurat (27)—with SAMap, a method developed specifically to facilitate cross-species single-cell transcriptomic comparisons (33). SAMap and Seurat results were generally consistent, yielding high alignment scores for cell types such as the *sst*⁺, *nos1*⁺, *chodl*⁺ interneurons, medial thalamic cell types, as well as cell types from the reticular thalamic nucleus and septum, cerebellar granule and Purkinje cells, and medium spiny neurons (figs. S9, A to D, S10, and S11).

Hence, even neuron types with considerable transcriptomic overlap between lizard and mouse show specific interspecies differences. This highlights the relevance of comprehensive transcriptomic characterization to identify common marker genes reliably, and the fact that “marker genes” commonly used for cell type identification in one species are not necessarily the most conserved ones. In turtle (12) and lizard, interneurons (INs) homologous to mouse parvalbumin (PV) INs do not express PV; their identification relies on different gene sets. “PV” labels are thus misnomers in reptiles; the terminology is inherited from earlier choices of markers specific to mammalian species. Finally, similar neuron types were not limited to subcortical regions; most brain divisions contained a mixture of similar and divergent neuron types (Fig. 3B).

Transcription factor codes common to lizard and mouse

To corroborate our findings and compare in detail neuron types in mouse and lizard, we selected scRNA-seq datasets with deeper cellular sampling and annotations from specific regions of the mouse brain: telencephalic GABAergic interneurons (34), thalamus (35), hypothalamus (36), and superior colliculus (37). For each of these four datasets, we performed joint CCA embedding on the above mouse cells and corresponding region-specific

subsets in lizard and clustered the joint embedding (Fig. 4), as introduced in Fig. 2A (see methods).

Lizard and mouse neurons were well integrated [see joint uniform manifold approximation and projection (UMAP) representations; Fig. 4, A to D]. For example, among telencephalic interneurons, we identified joint clusters belonging to the different subclasses derived from the medial ganglionic eminence (MGE) (*sst*, *pvalb*, and *chodl* in mouse) or caudal ganglionic eminence (CGE) (*sncg* and *vip* subclasses in mouse) (Fig. 4A and fig. S12, A and B), confirming and extending earlier results (12). In the hypothalamus, we found joint clusters of neurons from the ventromedial hypothalamus (VMH), paraventricular nuclei (PVN), arcuate nucleus, and other tuberal nuclei, as well as two other hypothalamic clusters that split mostly by neurotransmitter type (glutamate and GABA) (Fig. 4B and fig. S13, A and B). In the tectum (lizard optic tectum and mouse superior colliculus), integrated clusters grouped neurons by corresponding strata, or groups of layers (e.g., GABAergic interneurons in the superficial layers of both the superior colliculus and the optic tectum) (Fig. 4C and fig. S14, A and B). In the prethalamus and thalamus, joint clusters grouped the mouse reticular thalamic nucleus (RTn) with the lizard ventromedial thalamic nucleus (Vm), as well as glutamatergic neurons in the medial thalamus of both species, and in the lateral thalamus (Fig. 4D and fig. S15, A and B). These thalamic similarities between mouse and lizard are further examined below.

We next investigated the molecular signatures that underlie these similarities. We identified differentially expressed genes on species-specific datasets and intersected them in a cluster-specific manner across species, to point to common and thus potentially conserved marker genes. From these, we selected transcription factors to test whether integrated clusters can be defined by the combinatorial expression of transcription factors. Such common codes could be identified in many regions and neuronal populations (Fig. 4, E to H). For example, among telencephalic interneurons, mouse and lizard MGE-Sst and MGE-PV were both defined by the coexpression of *zeb2*, *mef2c*, *lhx6*, and *sox6* but differentiated by *pou3f3*, which is expressed only in MGE-Sst. MGE-Chodl cells from mouse and lizard were differentiated from other MGE-derived cell types by expression of *aff2* and lack of expression of *zeb2*; they could be further distinguished from CGE-derived cell types by coexpression of *lhx6*, *satb1*, and *sox6* (Fig. 4E).

In the hypothalamus, neurons from the ventromedial hypothalamus expressed *nr5a1*, *lef2*, *nr2f2*, and *isl1*, a gene combination common to

lizard and mouse that distinguished these neurons from the rest of the tuberal neurons (Fig. 4F). In the paraventricular hypothalamic nucleus, *nr4a1* differentiated two clusters by its expression (cluster 6) or absence of expression (cluster 5) (Fig. 4, B and F). Similarly shared transcription factor codes were found in the optic tectum/superior colliculus: In both species, GABAergic neurons from central layers were *zfhx4*⁺, *otx2*⁺, and *irx2*⁺, whereas those from superficial layers expressed the same three transcription factors plus *meis2* (Fig. 4G and fig. S16, A to D). Taken together, these examples indicate that evolutionarily conserved classes of neurons can be defined by the expression of a core set of transcription factors. In the thalamus and prethalamus, however, the results proved more complex, prompting us to analyze this region in greater detail (Fig. 4H).

Partial divergence of the thalamus between reptilian and mammalian lineages

The thalamus is a key diencephalic region positioned between the sensory-motor periphery and the cerebral cortex. Because the reptilian cerebral cortex retains ancestral characteristics (e.g., three rather than six layers, absence of sensory topography), examining the molecular organization of the thalamus in a reptile provides a distinctive opportunity to examine the potential coevolution of connected brain areas. Because the growth and complexification of the mammalian neocortex is reflected in a matching growth and complexification of the thalamus (38), we searched for molecular differences between thalamic neuron types in lizard and mouse.

We selected the 7721 lizard single neurons sampled from the thalamus, identified by a combination of dissection region and gene expression (*tcfl7l2*, *gbx2*, *lhx9*, or *foxp2* for glutamatergic clusters; *six3*, *meis2*, and *zic1* for GABAergic clusters; fig. S17, A to C). Of these, 4244 were glutamatergic (thalamus proper) neurons and 2617 were GABAergic (prethalamus) neurons (Fig. 5A). These single neurons could be grouped into 37 clusters, distinguished by specific combinations of marker genes (fig. S17A). We assigned each lizard neuron type to a thalamic nucleus by analyzing *in situ* hybridizations for cluster-specific or area-specific genes (e.g., transcription factors *tcfl7l2*, *zic1*, *foxp2*, or *gbx2*; effector genes such as *opn4*, expressed in dorsomedial thalamic neurons; *cbln1* in dorsolateral thalamic neurons; *vip* in neurons from the nucleus rotundus; and *sst2-like* in the ventromedial thalamic nuclei; 860 transcriptomes could not be assigned confidently to a thalamic nucleus) (Fig. 5B and fig. S17, B and C).

A principal components analysis (PCA) on the transcriptomes of lizard thalamic glutamatergic neurons revealed a clear segregation of medial (DMT1 to DMT4) and lateral

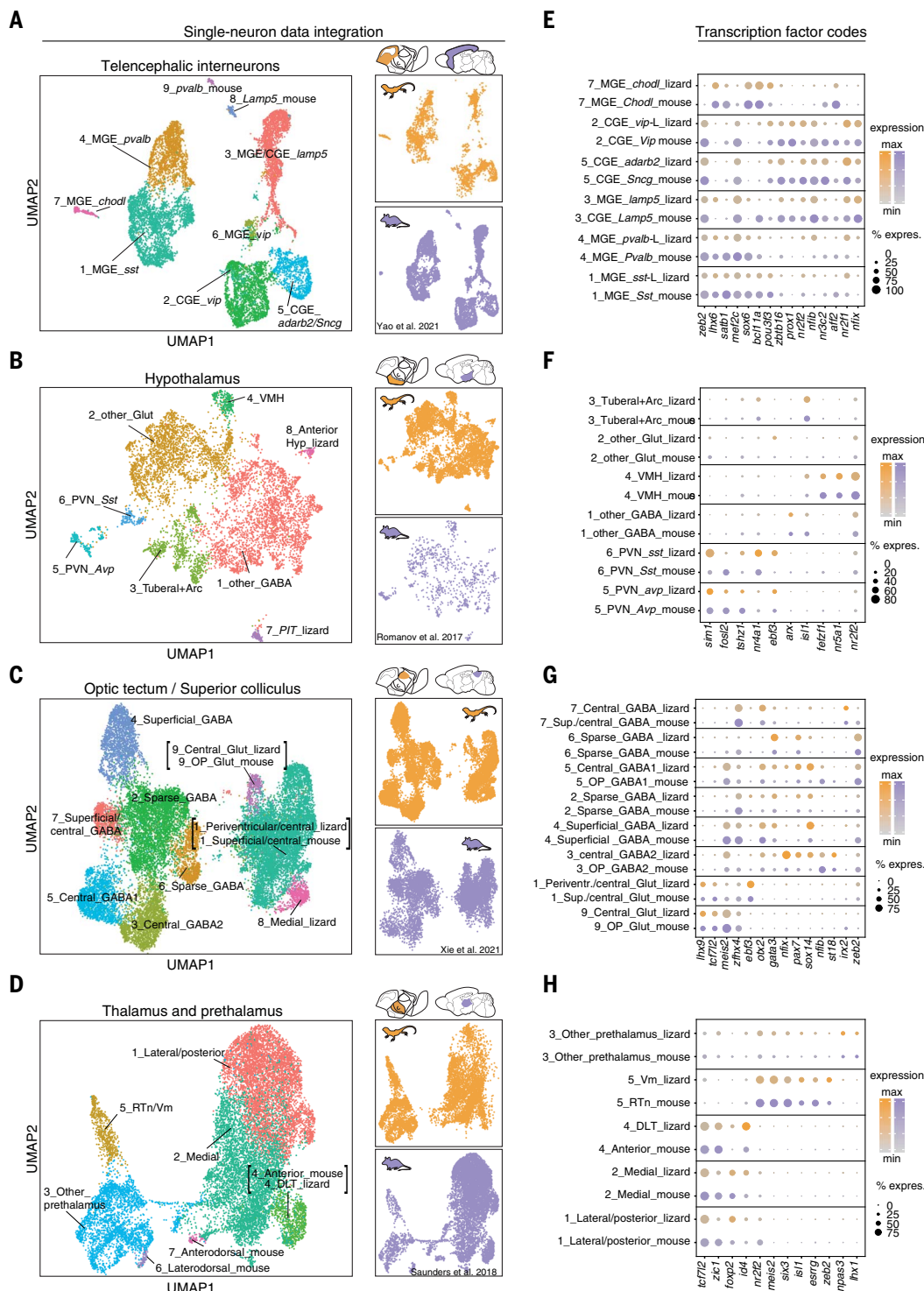


Fig. 4. Common transcription factor codes for identifiable neuron populations in lizard and mouse. (A to D) UMAP representations of integrated single-neuron transcriptomes from *Pogona* (this study) and mouse (34–37) (left), also shown by species of origin (right). Brain schematics show corresponding regions in mouse and lizard. (A) Telencephalic GABAergic interneurons (mouse: 8000 cells; lizard: 2599 cells). (B) Hypothalamic neurons (mouse: 772; lizard: 6221). (C) Optic tectum or superior colliculus (mouse: 8428; lizard: 13278). (D) Thalamic neurons (mouse: 8622; lizard: 6861). (E to H) Dot plots showing shared transcription factor codes for *Pogona* and mouse neuron types. Dot size represents fraction of neurons in a cluster that express the gene, and color intensity represents strength of expression.

thalamic clusters along the first principal component (PC1), confirmed by an analysis of the genes with highest absolute loadings on PC1 (Fig. 5, C and D). A similar finding was reported

in a mouse RNA-seq study of glutamatergic thalamic nuclei (39) and confirmed by joint analysis of mouse thalamic scRNA-seq data (26, 35, 39) (fig. S18A). To identify conserved

genes underlying this spatial segregation, we performed gene ontology analysis on the intersection of the 400 genes with highest absolute loadings on PC1 in each species (112 genes).

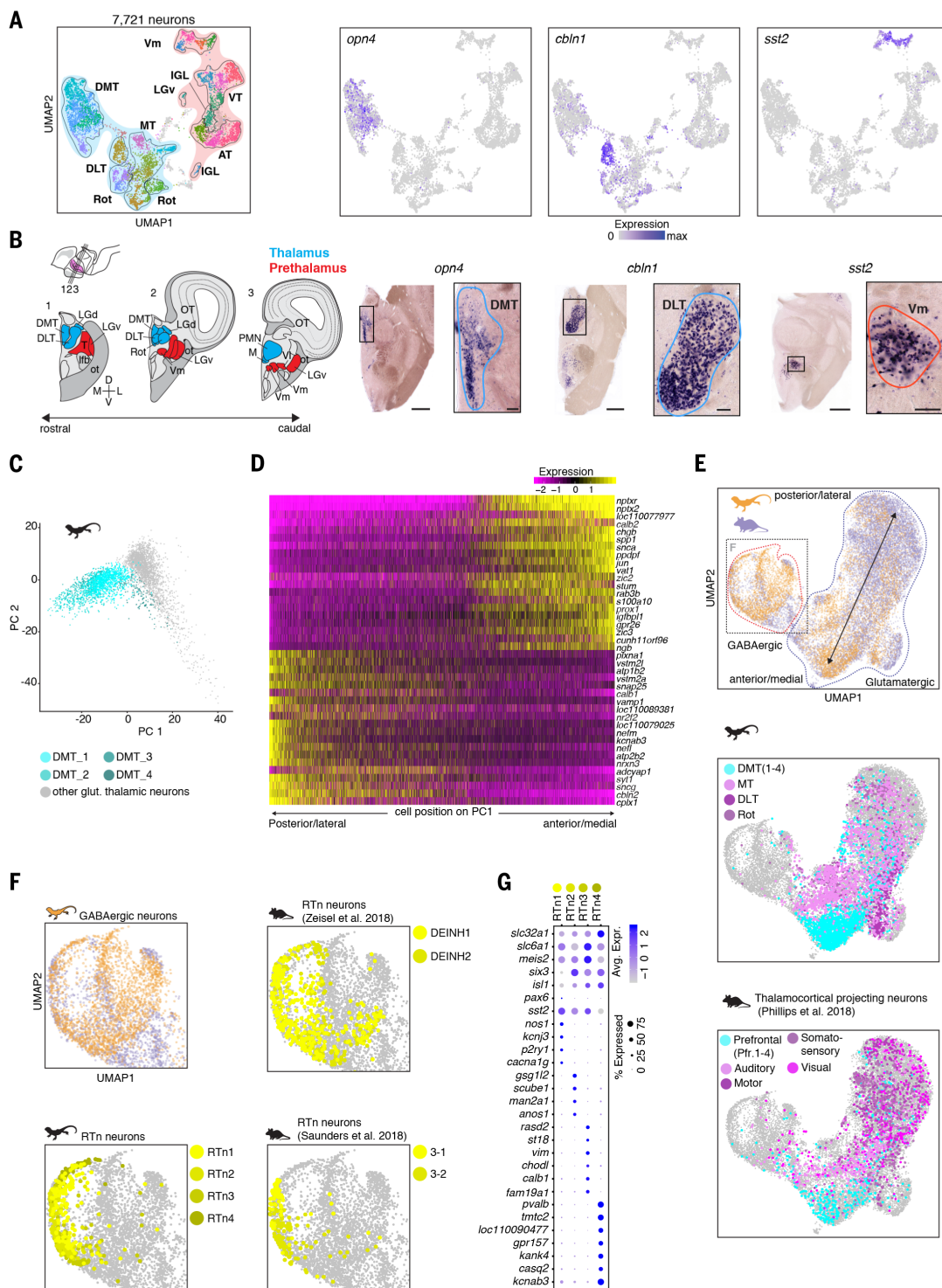


Fig. 5. Partial molecular and anatomical divergence of the thalamus between reptilian and mammalian lineages. (A) UMAP representation of 7721 neuronal single-neuron transcriptomes from the thalamus of *Pogona* colored by cluster [left; color shades as in (B)] showing the expression of *opn4*, *cbln1*, and *sst2-like* (right). MT, medial thalamic nucleus; DLT, dorsolateral thalamus; IGL, intergeniculate leaflet; Rot, nucleus rotundus; AT, anterior thalamus; VT, ventral thalamic nucleus; Vm, ventromedial thalamic nucleus. (B) Schematic of coronal sections of the lizard thalamus (left) showing glutamatergic (blue) and GABAergic (prethalamus, red) nuclei. Small schematic indicates coronal section planes. (Right) In situ hybridization

for *opn4* (expressed in DMT), *cbln1* (expressed in DLT), and *sst2-like* (expressed in Vm). Scale bar: 1 mm (main images) and 200 μ m (insets). **(C)** Projections of glutamatergic *Pogona* thalamus neurons in principal components 1 and 2 plane; DMT neurons are highlighted in cyan. **(D)** Heatmap of the top 40 genes with highest absolute loadings on principal component 1 (PC1); neurons sorted by PC1 score. **(E)** UMAP representation of 20,490 integrated single-neuron transcriptomes from *Pogona* and mouse thalamic datasets [mouse data from (26, 35, 39)]. Neurons colored by species of origin (top). UMAPs of integrated thalamic objects showing clusters of origin for *Pogona* (middle) and projection regions for mouse

[bottom; data from (39)]. (F) UMAP representations of integrated GABAergic neurons from mouse and *Pogona*. Color coded by species (top left: lizard, orange; mouse, purple), and by clusters of RTn neurons in the original datasets (top right, bottom left, and bottom right). (G) Dot plot showing

expression of genes defining the four subclusters (RTn1 to RTn4) of the lizard's reticular thalamic nucleus homolog. Dot size represents the fraction of cells in a given cluster that express the gene, and color intensity represents strength of expression.

This analysis revealed gene families related to calcium signaling, neural development, projections, and connectivity (fig. S18B) but only a small number of transcription factors. Taken together, these findings indicate that position along the mediolateral axis is a major correlate of thalamic neuronal diversity in amniotes and that a shared set of effector genes underlies this mediolateral distinction.

These observations were corroborated by an integrated analysis of 6861 lizard transcriptomes with 13,629 mouse single-cell transcriptomes (see methods) from the mouse thalamus and prethalamus (Fig. 5E and fig. S19, A and B). For this analysis, we used the previously mentioned mouse datasets (26, 35, 39), including data from a study where mouse thalamic neurons with distinct projections to cortex were sampled after retrograde tracing from different cortical areas (39). This enabled us to compare these projection types with those of lizard thalamic neurons whose targets have been described (40–44). The cross-species data integration recapitulated our observations from the PCA analysis. Glutamatergic neurons co-clustered in two broad classes, according to their position along the mediolateral axis.

Lizard neurons from the dorsomedial thalamus (DMT), a nucleus that projects to limbic areas in lizards (40, 41), co-clustered with mouse thalamic neurons that project to the prefrontal cortex [Pfr:4 and Pfr:3 from (39)]. On the basis of gene expression and connectivity, these mouse neurons likely originated from the paraventricular nucleus and other medial nuclei that project to prefrontal and limbic areas (45) in mammals (Fig. 5E and fig. S19A).

A second class of thalamic glutamatergic neurons included neurons from sensory relay nuclei, but with an intermingling of sensory modalities (fig. S19A). The lateral or posterior nuclei in lizard include the nucleus rotundus, the dorsolateral thalamic nucleus and, in a more caudal position, the so-called nucleus medialis. The nucleus rotundus is typically compared to the mammalian pulvinar because both relay visual information from the optic tectum/superior colliculus to the pallium (46); the nucleus medialis relays auditory and somatosensory inputs (42, 43), whereas the dorsolateral thalamic nucleus is multimodal (44). In mammals, many of these lateral or posterior thalamic nuclei are connected to topologically ordered sensory areas of the mammalian neocortex that have no clear reptilian equivalent. The absence of co-clustering of lizard and mouse thalamic neurons by modality suggests that the diversification of cell

types in the lateral or posterior thalamus may be related to the divergent fates of the cortex in the mammalian and reptilian lineages, and particularly to the prominent expansion of the cerebral cortex in mammals.

In mammals, the excitatory thalamocortical loops, which reciprocally connect pairs of dorsal thalamic nuclei and cortical regions, rely on the GABAergic neurons of the RTn for inhibitory control and modulation. This negative feedback, connecting reticular thalamic nucleus interneurons to glutamatergic projection neurons within the thalamus, plays important roles in the generation of spindles and slow oscillations during sleep (47–49).

Not much is known about the existence of a reticular thalamic nucleus homolog in reptiles. There is as yet no evidence for sleep spindle oscillations in lizard (50), but immunocytochemical and connectivity studies have suggested that the turtle anterior entopeduncular nucleus (51), the lizard ventromedial thalamic nuclei (52), and the caiman reticular thalamic nucleus (53) could be homologs of the mammalian reticular thalamic nucleus.

Our data revealed that neurons from the lizard ventromedial thalamic nucleus form four separable transcriptomic clusters, and that together they co-cluster with the mouse RTn (Fig. 5F and fig. S19B). In both species, those neuron types had similar transcription factor expression profiles (expression of *six3*, *meis2*, and *isl1*, and absence of *pax6*) and shared expression of the ion-channel genes *cacna1i*, *kcnip1*, and other effector genes (54) (Fig. 5G and fig. S19C). In *Pogona* and other reptiles (55), these neurons are close to the lateral forebrain bundle, a position shared with mammals, suggesting a similar relationship with the forebrain. Our data thus suggest that the lizard ventromedial thalamic nucleus is a homolog of the mammalian RTn.

Discussion

The contrast between the conservation of early developmental regions and the diversity of neural cytoarchitectonics and connectivity of vertebrate brains has engendered competing views on brain evolution (56). Our data indicate that neuronal transcriptomes carry molecular signatures of developmental and evolutionary history as well as connectivity, suggesting that a systematic comparison of single-cell transcriptomes across species can bridge earlier types of comparisons in brain evolution studies (57–59). The existence of broad classes of neurons shared by a reptile and a mammal, identified here as joint clus-

ters of lizard and mouse neurons (Figs. 2 and 4), indicates that the broadly defined brain regions of amniotes are organized into smaller units with molecular similarity across species. As suggested by the conserved expression of homeodomain-type transcription factors, these classes might correspond to the adult derivatives of the embryonic prosomeres, units of embryonic progenitors conserved in vertebrate species (3). It has been noticed that the conservation of vertebrate brain regions correlates with the conservation of mesoscale connectivity (60, 61); we suggest that those genes related to connectivity (e.g., axonal pathfinding, surface molecules, etc.) with conserved expression in neuron classes may be functionally implicated in the establishment of evolutionarily conserved patterns of mesoscale connectivity.

At finer resolution, however, the comparison of neuron types challenges the assumption that certain brain regions are more conserved than others. In the telencephalon, diencephalon, and mesencephalon—our sampling of the hindbrain was limited mainly to the cerebellum—we found broad distributions of cell type projection scores (Fig. 3B). While some neuron types could be mapped with confidence from lizard to mouse, many others could not, owing to wide molecular divergence. We interpret these varying degrees of molecular divergence as the results of partial diversification and specialization of neuron types in either or both lineages.

Did common traits link neuron types with similar transcriptomes across the two examined species? Such neuron types were found in the telencephalon, diencephalon, and mesencephalon; they could be local (e.g., reticular thalamic nucleus or pallial GABAergic neurons) or long-range projecting (e.g., striatal medium spiny neurons); and they were not limited to one neurotransmitter type. Thus, the degree of molecular divergence of neuron types could be predicted neither from their developmental origin nor from their phenotypes (neurotransmitter, local versus long-range projection). We propose that, while strong developmental constraints in early embryogenesis underlie the conservation of broad classes of neurons, the development and evolution of specific types and subtypes is more plastic. Neuron types might be deeply conserved if they happen to express genes under stronger pleiotropic constraints, as in the cerebellum (62). Alternatively, neurons could be under strong selective pressure for their singular function in neural circuit motifs. Likewise,

functional constraints may also lead to the convergent evolution of neuronal transcriptomes, as in the case of the reptilian dorsal ventricular ridge and mammalian cerebral cortex (12).

As an extreme example, the thalamic complex provides some indications on the potential drivers of the evolutionary diversification of neurons. The existence of a conserved reticular thalamic nucleus (GABAergic, prethalamic), which occupies a key role in thalamocortical connectivity and dynamics in mammals, suggests that some aspects of the organization of thalamocortical circuits may trace back to amniote ancestors (51, 53). However, similarities between mouse and lizard are less sharp for glutamatergic neurons. On the basis of their shared transcriptomic variation, lizard and mouse thalamic glutamatergic neurons could be grouped into only two large classes, medial and lateral, indicating that other dimensions of thalamic organization (sensory modality, core versus matrix, etc.) are not encoded by the same sets of genes across species. Lizard and mouse neurons that co-clustered as “medial thalamus” both project to limbic areas in the pallium and subpallium, supporting the hypothesis that mammalian medial nuclei (including the paraventricular nucleus) and the reptilian dorsomedial thalamus are homologous (fig. S20) (63–65). In the “lateral thalamus,” lizard and mouse neurons did not co-cluster by sensory modality. This might be explained by transient expression of conserved modality-specific genes only during development. Alternatively, the identity of sensory relay nuclei might not be encoded by conserved transcriptional programs in lizard and mouse, suggesting that modality-specific programs would have evolved independently in reptiles and mammals. Consistent with this, the primary sensory areas in the cerebral cortex that are connected to lateral thalamic relay nuclei underwent, in the evolutionary line leading to mammals, profound changes that are specific to them. The parallel diversification of thalamic and cortical neuron types suggests that thalamocortical circuits evolved in amniotes by duplication and divergence, following a principle similar to that proposed for the evolution of cerebellar nuclei (59).

Hence, even though lizard and mouse diverged more than 300 million years ago, neuron types in their brains can be assigned to conserved classes, reflecting the existence of shared developmental programs that establish vertebrate brain regions. However, further diversity and molecular heterogeneity within each of these classes indicates that neuronal identities evolve under selective pressures that act globally on the brain, regardless of developmental origin. Extending comparative transcriptomics investigations to other species should provide insights about

the processes that enabled the adaptation of vertebrates to different environments over the past 550 million years.

Materials and methods summary

Single-cell RNA sequencing

For single-cell RNA sequencing, cells were prepared by dissociating microdissected brain regions from adult *P. vitticeps* as described previously (25). The single-cell suspension was used to generate scRNA-seq libraries using the 10X Genomics Chromium Single Cell 3' Reagent Kit (v2 and v3 chemistry) and sequenced with Illumina NextSeq 500 according to the manufacturer's protocols. The resulting scRNA-seq data were aligned with CellRanger v3.0 and processed using Seurat v3.1. Analysis steps included a first filtering of low-quality cells on the basis of the number of genes expressed per cell (v2: >400 genes per cell; v3: >800 genes per cell) and then normalized, scaled, dimensionality-reduced with PCA and Louvain-clustered. This revealed a cluster of low-quality cells by a combination of features (no. of genes expressed per cell, no. of unique molecular identifiers per cell, percentage of mitochondrial genes per cell, and percentage of rRNAs per cell). A support vector machine (SVM) was then trained to distinguish high- and low-quality cells by these features, and the data were further filtered by removing cells identified as low-quality by the SVM. The remaining high-quality cells (285,483) were processed similarly to reveal major cell classes. We identified neuronal clusters among the major cell classes by their expression of marker genes (e.g., *snap25*), extracted them computationally, filtered further to >1000 genes per cell and, after several rounds of clustering and removal of low-quality clusters (according to the above criteria), ended up with 89,015 neuronal transcriptomes.

Cross-species comparisons

For cross-species comparisons, we used previously published datasets from mice containing cells from the whole brain (26) or region-specific subsets (34–37, 39). For embeddings of specific regions, the lizard data were first subsetted to contain only cells from matching brain regions. We then used Seurat v3.1 for joint CCA embedding of mouse and lizard single cells, using only genes that were annotated as one-to-one orthologs between mouse and *Pogona* by Ensembl. We also validated some of the results obtained by this approach using SAMap (33), a method specifically designed for cross-species integration of scRNA-seq data. For this, we first constructed BLAST maps between the proteomes of *Pogona* and mouse.

Histology

To prepare probes for *in situ* hybridization, we either PCR-amplified fragments of genes

of interest from *P. vitticeps* cDNA libraries, as previously described (12), or ordered as gene fragments with 31-base pair overhangs on both ends that were overlapping with the pCRII-TOPO vector. Gene fragments were then cloned into the pCRII vector using either the TA Cloning Kit (Invitrogen) or the Gibson Assembly Cloning Kit (New England Biolabs) according to each manufacturer's protocol. Clones were verified by Sanger sequencing, and DIG- or FITC-labeled probes were transcribed *in vitro* and purified, and a chromogenic *in situ* hybridization protocol was followed as described previously (12). After mounting, sections were imaged at 20 \times magnification using an automatic digital slide scanner (Pannoramic MIDI II, 3DHISTECH).

REFERENCES AND NOTES

1. P. S. Katz, Phylogenetic plasticity in the evolution of molluscan neural circuits. *Curr. Opin. Neurobiol.* **41**, 8–16 (2016). doi: [10.1016/j.conb.2016.07.004](https://doi.org/10.1016/j.conb.2016.07.004); pmid: [27455462](https://pubmed.ncbi.nlm.nih.gov/27455462/)
2. L. Puelles, M. Harrison, G. Paxinos, C. Watson, A developmental ontology for the mammalian brain based on the prosomeric model. *Trends Neurosci.* **36**, 570–578 (2013). doi: [10.1016/j.tins.2013.06.004](https://doi.org/10.1016/j.tins.2013.06.004); pmid: [23871546](https://pubmed.ncbi.nlm.nih.gov/23871546/)
3. L. Puelles, “Plan of the developing vertebrate nervous system: Relating embryology to the adult nervous system (prosomere model, overview of brain organization)” in *Patterning and Cell Type Specification in the Developing CNS and PNS*, J. Rubenstein, P. Rakic, Eds. (Elsevier, 2013), pp. 187–209.
4. R. Nieuwenhuys, Principles of current vertebrate neuromorphology. *Brain Behav. Evol.* **90**, 117–130 (2017). doi: [10.1159/000460237](https://doi.org/10.1159/000460237); pmid: [28988231](https://pubmed.ncbi.nlm.nih.gov/28988231/)
5. A. B. Butler, The evolution of the dorsal thalamus of jawed vertebrates, including mammals: Cladistic analysis and a new hypothesis. *Brain Res. Brain Res. Rev.* **19**, 29–65 (1994). doi: [10.1016/0165-0173\(94\)90003-5](https://doi.org/10.1016/0165-0173(94)90003-5); pmid: [8167659](https://pubmed.ncbi.nlm.nih.gov/8167659/)
6. G. F. Striedter, The telencephalon of tetrapods in evolution. *Brain Behav. Evol.* **49**, 179–194 (1997). doi: [10.1159/000112991](https://doi.org/10.1159/000112991); pmid: [9096908](https://pubmed.ncbi.nlm.nih.gov/9096908/)
7. E. R. Chapman, S. An, N. Barton, R. Jahn, SNAP-25, a t-SNARE which binds to both syntaxin and synaptobrevin via domains that may form coiled coils. *J. Biol. Chem.* **269**, 27427–27432 (1994). doi: [10.1016/S0021-9258\(18\)47003-2](https://doi.org/10.1016/S0021-9258(18)47003-2); pmid: [7961655](https://pubmed.ncbi.nlm.nih.gov/7961655/)
8. L. Claesson-Welsh, A. Hammacher, B. Westermark, C. H. Heldin, M. Nistér, Identification and structural analysis of the A type receptor for platelet-derived growth factor. Similarities with the B type receptor. *J. Biol. Chem.* **264**, 1742–1747 (1989). doi: [10.1016/S0021-9258\(18\)94249-3](https://doi.org/10.1016/S0021-9258(18)94249-3); pmid: [2536372](https://pubmed.ncbi.nlm.nih.gov/2536372/)
9. Y. Chen et al., The oligodendrocyte-specific G protein-coupled receptor GPR17 is a cell-intrinsic timer of myelination. *Nat. Neurosci.* **12**, 1398–1406 (2009). doi: [10.1038/nn.2410](https://doi.org/10.1038/nn.2410); pmid: [19838178](https://pubmed.ncbi.nlm.nih.gov/19838178/)
10. R. H. Quarles, Myelin-associated glycoprotein (MAG): Past, present and beyond. *J. Neurochem.* **100**, 1431–1448 (2007). doi: [10.1111/j.1471-4159.2006.04319.x](https://doi.org/10.1111/j.1471-4159.2006.04319.x); pmid: [17241126](https://pubmed.ncbi.nlm.nih.gov/17241126/)
11. C. Yanes, M. Monzon-Mayor, M. S. Ghandour, J. de Barry, G. Gombos, Radial glia and astrocytes in developing and adult telencephalon of the lizard *Gallotia galloti* as revealed by immunohistochemistry with anti-GFAP and anti-vimentin antibodies. *J. Comp. Neurol.* **295**, 559–568 (1990). doi: [10.1002/cne.902950405](https://doi.org/10.1002/cne.902950405); pmid: [2358521](https://pubmed.ncbi.nlm.nih.gov/2358521/)
12. M. A. Tosches et al., Evolution of pallium, hippocampus, and cortical cell types revealed by single-cell transcriptomics in reptiles. *Science* **360**, 881–888 (2018). doi: [10.1126/science.aar4237](https://doi.org/10.1126/science.aar4237); pmid: [29724907](https://pubmed.ncbi.nlm.nih.gov/29724907/)
13. S. M. Islam et al., Draxin, a repulsive guidance protein for spinal cord and forebrain commissures. *Science* **323**, 388–393 (2009). doi: [10.1126/science.1165187](https://doi.org/10.1126/science.1165187); pmid: [19150847](https://pubmed.ncbi.nlm.nih.gov/19150847/)
14. S. Gobron et al., SCO-spondin is evolutionarily conserved in the central nervous system of the chordate phylum. *Neuroscience* **88**, 655–664 (1999). doi: [10.1016/S0306-4522\(98\)00252-8](https://doi.org/10.1016/S0306-4522(98)00252-8); pmid: [10197783](https://pubmed.ncbi.nlm.nih.gov/10197783/)

15. A. Paul *et al.*, Transcriptional architecture of synaptic communication delineates GABAergic neuron identity. *Cell* **171**, 522–539.e20 (2017). doi: [10.1016/j.cell.2017.08.032](https://doi.org/10.1016/j.cell.2017.08.032); pmid: [28942923](https://pubmed.ncbi.nlm.nih.gov/28942923/)
16. S. J. Smith *et al.*, Single-cell transcriptomic evidence for dense intracortical neuropeptide networks. *eLife* **8**, e47889 (2019). doi: [10.7554/eLife.47889](https://doi.org/10.7554/eLife.47889); pmid: [31710287](https://pubmed.ncbi.nlm.nih.gov/31710287/)
17. S. R. Taylor *et al.*, Molecular topography of an entire nervous system. *Cell* **184**, 4329–4347.e23 (2021). doi: [10.1016/j.cell.2021.06.023](https://doi.org/10.1016/j.cell.2021.06.023); pmid: [34237253](https://pubmed.ncbi.nlm.nih.gov/34237253/)
18. T. Kumamoto, C. Hanashima, Evolutionary conservation and conversion of Foxg1 function in brain development. *Dev. Growth Differ.* **59**, 258–269 (2017). doi: [10.1111/dgd.12367](https://doi.org/10.1111/dgd.12367); pmid: [28581027](https://pubmed.ncbi.nlm.nih.gov/28581027/)
19. A. Nagalski *et al.*, Molecular anatomy of the thalamic complex and the underlying transcription factors. *Brain Struct. Funct.* **221**, 2493–2510 (2016). doi: [10.1007/s00429-015-1052-5](https://doi.org/10.1007/s00429-015-1052-5); pmid: [25963709](https://pubmed.ncbi.nlm.nih.gov/25963709/)
20. E. Desfilis, A. Abellán, V. Sentandreu, L. Medina, Expression of regulatory genes in the embryonic brain of a lizard and implications for understanding pallial organization and evolution. *J. Comp. Neurol.* **526**, 166–202 (2018). doi: [10.1002/cne.24329](https://doi.org/10.1002/cne.24329); pmid: [28891227](https://pubmed.ncbi.nlm.nih.gov/28891227/)
21. J. Aruga *et al.*, Mouse Zic1 is involved in cerebellar development. *J. Neurosci.* **18**, 284–293 (1998). doi: [10.1523/JNEUROSCI.18-01-00284.1998](https://doi.org/10.1523/JNEUROSCI.18-01-00284.1998); pmid: [9412507](https://pubmed.ncbi.nlm.nih.gov/9412507/)
22. I. Bachy, J. Berthon, S. Rétaux, Defining pallial and subpallial divisions in the developing *Xenopus* forebrain. *Mech. Dev.* **117**, 163–172 (2002). doi: [10.1016/S0925-4773\(02\)00199-5](https://doi.org/10.1016/S0925-4773(02)00199-5); pmid: [12204256](https://pubmed.ncbi.nlm.nih.gov/12204256/)
23. R. F. Leung *et al.*, Genetic regulation of vertebrate forebrain development by homeobox genes. *Front. Neurosci.* **16**, 843794 (2022). doi: [10.3389/fnins.2022.843794](https://doi.org/10.3389/fnins.2022.843794); pmid: [35546872](https://pubmed.ncbi.nlm.nih.gov/35546872/)
24. C. E. Love, V. E. Prince, Expression and retinoic acid regulation of the zebrafish nr2f orphan nuclear receptor genes. *Dev. Dyn.* **241**, 1603–1615 (2012). doi: [10.1002/dvdy.23838](https://doi.org/10.1002/dvdy.23838); pmid: [22836912](https://pubmed.ncbi.nlm.nih.gov/22836912/)
25. H. Norimoto *et al.*, A claustrum in reptiles and its role in slow-wave sleep. *Nature* **578**, 413–418 (2020). doi: [10.1038/s41586-020-1993-6](https://doi.org/10.1038/s41586-020-1993-6); pmid: [32051589](https://pubmed.ncbi.nlm.nih.gov/32051589/)
26. A. Zeisel *et al.*, Molecular architecture of the mouse nervous system. *Cell* **174**, 999–1014.e22 (2018). doi: [10.1016/j.cell.2018.06.021](https://doi.org/10.1016/j.cell.2018.06.021); pmid: [30096314](https://pubmed.ncbi.nlm.nih.gov/30096314/)
27. T. Stuart *et al.*, Comprehensive integration of single-cell data. *Cell* **177**, 1888–1902.e2 (2019). doi: [10.1016/j.cell.2019.05.031](https://doi.org/10.1016/j.cell.2019.05.031); pmid: [3117818](https://pubmed.ncbi.nlm.nih.gov/3117818/)
28. R. Nieuwenhuys, L. Puelles, *Towards a New Neuromorphology* (Springer International Publishing, Cham, 2016).
29. T. E. Bakken *et al.*, Comparative cellular analysis of motor cortex in human, marmoset and mouse. *Nature* **598**, 111–119 (2021). doi: [10.1038/s41586-021-03465-8](https://doi.org/10.1038/s41586-021-03465-8); pmid: [34616062](https://pubmed.ncbi.nlm.nih.gov/34616062/)
30. E. Rueda-Alaña, F. García-Moreno, Time in neurogenesis: Conservation of the developmental formation of the cerebellar circuitry. *Brain Behav. Evol.* **97**, 33–47 (2022). doi: [10.1159/000519068](https://doi.org/10.1159/000519068); pmid: [34592741](https://pubmed.ncbi.nlm.nih.gov/34592741/)
31. M. Stephenson-Jones, E. Samuelsson, J. Ericsson, B. Robertson, S. Grillner, Evolutionary conservation of the basal ganglia as a common vertebrate mechanism for action selection. *Curr. Biol.* **21**, 1081–1091 (2011). doi: [10.1016/j.cub.2011.05.001](https://doi.org/10.1016/j.cub.2011.05.001); pmid: [21700460](https://pubmed.ncbi.nlm.nih.gov/21700460/)
32. L. Freudenmacher, A. von Twickel, W. Walkowiak, The habenula as an evolutionary conserved link between basal ganglia, limbic, and sensory systems—A phylogenetic comparison based on anuran amphibians. *J. Comp. Neurol.* **528**, 705–728 (2020). doi: [10.1002/cne.24777](https://doi.org/10.1002/cne.24777); pmid: [31566737](https://pubmed.ncbi.nlm.nih.gov/31566737/)
33. A. J. Tarashansky *et al.*, Mapping single-cell atlases throughout Metazoa unravels cell type evolution. *eLife* **10**, e66747 (2021). doi: [10.7554/eLife.66747](https://doi.org/10.7554/eLife.66747); pmid: [33944782](https://pubmed.ncbi.nlm.nih.gov/33944782/)
34. Z. Yao *et al.*, A taxonomy of transcriptomic cell types across the isocortex and hippocampal formation. *Cell* **184**, 3222–3241.e26 (2021). doi: [10.1016/j.cell.2021.04.021](https://doi.org/10.1016/j.cell.2021.04.021); pmid: [34004146](https://pubmed.ncbi.nlm.nih.gov/34004146/)
35. A. Saunders *et al.*, Molecular diversity and specializations among the cells of the adult mouse brain. *Cell* **174**, 1015–1030.e16 (2018). doi: [10.1016/j.cell.2018.07.028](https://doi.org/10.1016/j.cell.2018.07.028); pmid: [30096299](https://pubmed.ncbi.nlm.nih.gov/30096299/)
36. R. A. Romanov *et al.*, Molecular interrogation of hypothalamic organization reveals distinct dopamine neuronal subtypes. *Nat. Neurosci.* **20**, 176–188 (2017). doi: [10.1038/nn.4462](https://doi.org/10.1038/nn.4462); pmid: [27991900](https://pubmed.ncbi.nlm.nih.gov/27991900/)
37. Z. Xie *et al.*, Transcriptomic encoding of sensorimotor transformation in the midbrain. *eLife* **10**, e69825 (2021). doi: [10.7554/eLife.69825](https://doi.org/10.7554/eLife.69825); pmid: [34318750](https://pubmed.ncbi.nlm.nih.gov/34318750/)
38. A. C. Halley, L. Krubitzer, Not all cortical expansions are the same: The coevolution of the neocortex and the dorsal thalamus in mammals. *Curr. Opin. Neurobiol.* **56**, 78–86 (2019). doi: [10.1016/j.conb.2018.12.003](https://doi.org/10.1016/j.conb.2018.12.003); pmid: [30658218](https://pubmed.ncbi.nlm.nih.gov/30658218/)
39. J. W. Phillips *et al.*, A repeated molecular architecture across thalamic pathways. *Nat. Neurosci.* **22**, 1925–1935 (2019). doi: [10.1038/s41593-019-0483-3](https://doi.org/10.1038/s41593-019-0483-3); pmid: [31527803](https://pubmed.ncbi.nlm.nih.gov/31527803/)
40. L. L. Bruce, A. B. Butler, Telencephalic connections in lizards. I. Projections to cortex. *J. Comp. Neurol.* **229**, 585–601 (1984). doi: [10.1002/cne.90229011](https://doi.org/10.1002/cne.90229011); pmid: [6209313](https://pubmed.ncbi.nlm.nih.gov/6209313/)
41. C. Font, A. Martínez-Marcos, A. Lanuza, P. V. Hoogland, F. Martínez-García, Septal complex of the telencephalon of the lizard *Podarcis hispanica*. II. Afferent connections. *J. Comp. Neurol.* **383**, 489–511 (1997). doi: [10.1002/\(SICI\)1096-9861\(19970714\)383:4<489::AID-CNE7>3.0.CO;2-Z](https://doi.org/10.1002/(SICI)1096-9861(19970714)383:4<489::AID-CNE7>3.0.CO;2-Z); pmid: [9208995](https://pubmed.ncbi.nlm.nih.gov/9208995/)
42. R. E. Foster, W. C. Hall, The organization of central auditory pathways in a reptile, *Iguana iguana*. *J. Comp. Neurol.* **178**, 783–831 (1978). doi: [10.1002/cne.901780412](https://doi.org/10.1002/cne.901780412); pmid: [632382](https://pubmed.ncbi.nlm.nih.gov/632382/)
43. M. B. Pritz, M. E. Stritzel, Anatomical identification of a telencephalic somatosensory area in a reptile, *Caiman crocodilus*. *Brain Behav. Evol.* **43**, 107–127 (1994). doi: [10.1159/000113628](https://doi.org/10.1159/000113628); pmid: [8143143](https://pubmed.ncbi.nlm.nih.gov/8143143/)
44. E. Desfilis, E. Font, M. Belekhova, N. Kenigfest, Afferent and efferent projections of the dorsal anterior thalamic nuclei in the lizard *Podarcis hispanica* (Sauria, Lacertidae). *Brain Res. Bull.* **57**, 447–450 (2002). doi: [10.1016/S0361-9230\(01\)00727-4](https://doi.org/10.1016/S0361-9230(01)00727-4); pmid: [11923008](https://pubmed.ncbi.nlm.nih.gov/11923008/)
45. G. J. Kirouac, Placing the paraventricular nucleus of the thalamus within the brain circuits that control behavior. *Neurosci. Biobehav. Rev.* **56**, 315–329 (2015). doi: [10.1016/j.neubiorev.2015.08.005](https://doi.org/10.1016/j.neubiorev.2015.08.005); pmid: [26255593](https://pubmed.ncbi.nlm.nih.gov/26255593/)
46. J. C. Dávila, M. J. Andreu, M. A. Real, L. Puelles, S. Guirado, Mesencephalic and diencephalic afferent connections to the thalamic nucleus rotundus in the lizard, *Psammmodromus algirus*. *Eur. J. Neurosci.* **16**, 267–282 (2002). doi: [10.1046/j.1460-9568.2002.02091x](https://doi.org/10.1046/j.1460-9568.2002.02091x); pmid: [12169109](https://pubmed.ncbi.nlm.nih.gov/12169109/)
47. D. Contreras, M. Steriade, Cellular basis of EEG slow rhythms: A study of dynamic corticothalamic relationships. *J. Neurosci.* **15**, 604–622 (1995). doi: [10.1523/JNEUROSCI.15-01-00604.1995](https://doi.org/10.1523/JNEUROSCI.15-01-00604.1995); pmid: [7823167](https://pubmed.ncbi.nlm.nih.gov/7823167/)
48. M. Steriade, D. A. McCormick, T. J. Sejnowski, Thalamocortical oscillations in the sleeping and aroused brain. *Science* **262**, 679–685 (1993). doi: [10.1126/science.8235588](https://doi.org/10.1126/science.8235588); pmid: [8235588](https://pubmed.ncbi.nlm.nih.gov/8235588/)
49. M. Steriade, L. Domich, G. Oakson, M. Deschénes, The deafferented reticular thalamic nucleus generates spindle rhythmicity. *J. Neurophysiol.* **57**, 260–273 (1987). doi: [10.1152/jn.1987.57.1.260](https://doi.org/10.1152/jn.1987.57.1.260); pmid: [3559675](https://pubmed.ncbi.nlm.nih.gov/3559675/)
50. M. Shein-Idelson, J. M. Ondracek, H.-P. Liaw, S. Reiter, G. Laurent, Slow waves, sharp waves, ripples, and REM in sleeping dragons. *Science* **352**, 590–595 (2016). doi: [10.1126/science.aaf3621](https://doi.org/10.1126/science.aaf3621); pmid: [27126045](https://pubmed.ncbi.nlm.nih.gov/27126045/)
51. N. Kenigfest *et al.*, The turtle thalamic anterior entopeduncular nucleus shares connectional and neurochemical characteristics with the mammalian thalamic reticular nucleus. *J. Chem. Neuroanat.* **30**, 129–143 (2005). doi: [10.1016/j.jchemneu.2005.07.001](https://doi.org/10.1016/j.jchemneu.2005.07.001); pmid: [16140498](https://pubmed.ncbi.nlm.nih.gov/16140498/)
52. C. Díaz, C. Yanés, C. M. Trujillo, L. Puelles, The leteridian reticular thalamic nucleus projects topographically upon the dorsal thalamus: Experimental study in *Gallotia galloti*. *J. Comp. Neurol.* **343**, 193–208 (1994). doi: [10.1002/cne.903430202](https://doi.org/10.1002/cne.903430202); pmid: [8027439](https://pubmed.ncbi.nlm.nih.gov/8027439/)
53. M. B. Pritz, M. E. Stritzel, A different type of vertebrate thalamic organization. *Brain Res.* **525**, 330–334 (1990). doi: [10.1016/0006-8993\(90\)90885-F](https://doi.org/10.1016/0006-8993(90)90885-F); pmid: [1701334](https://pubmed.ncbi.nlm.nih.gov/1701334/)
54. Y. Li *et al.*, Distinct subnetworks of the thalamic reticular nucleus. *Nature* **583**, 819–824 (2020). doi: [10.1038/s41586-020-2504-5](https://doi.org/10.1038/s41586-020-2504-5); pmid: [32699411](https://pubmed.ncbi.nlm.nih.gov/32699411/)
55. M. B. Pritz, Thalamic reticular nucleus in *Alligator mississippiensis*: Soma and dendritic morphology. *J. Comp. Neurol.* **529**, 3785–3844 (2021). doi: [10.1002/cne.25194](https://doi.org/10.1002/cne.25194); pmid: [34031891](https://pubmed.ncbi.nlm.nih.gov/34031891/)
56. M. A. Tosches, From cell types to an integrated understanding of brain evolution: The case of the cerebral cortex. *Annu. Rev. Cell Dev. Biol.* **37**, 495–517 (2021). doi: [10.1146/annurev-cellbio-120319-112654](https://doi.org/10.1146/annurev-cellbio-120319-112654); pmid: [34416113](https://pubmed.ncbi.nlm.nih.gov/34416113/)
57. M. E. R. Shafer, A. N. Sawh, A. F. Schier, Gene family evolution underlies cell-type diversification in the hypothalamus of teleosts. *Nat. Ecol. Evol.* **6**, 63–76 (2022). doi: [10.1038/s41559-021-01580-3](https://doi.org/10.1038/s41559-021-01580-3); pmid: [34824389](https://pubmed.ncbi.nlm.nih.gov/34824389/)
58. B. M. Colquitt, D. P. Merullo, G. Konopka, T. F. Roberts, M. S. Brainard, Cellular transcriptomics reveals evolutionary identities of songbird vocal circuits. *Science* **371**, eabd9704 (2021). doi: [10.1126/science.abd9704](https://doi.org/10.1126/science.abd9704); pmid: [33574185](https://pubmed.ncbi.nlm.nih.gov/33574185/)
59. J. M. Kebischull *et al.*, Cerebellar nuclei evolved by repeatedly duplicating a conserved cell-type set. *Science* **370**, eabd5059 (2020). doi: [10.1126/science.abd5059](https://doi.org/10.1126/science.abd5059); pmid: [33335034](https://pubmed.ncbi.nlm.nih.gov/33335034/)
60. S. M. Suryanarayana, J. Pérez-Fernández, B. Robertson, S. Grillner, The lamprey forebrain – evolutionary implications. *Brain Behav. Evol.* **96**, 318–333 (2022). doi: [10.1159/000517492](https://doi.org/10.1159/000517492); pmid: [34192700](https://pubmed.ncbi.nlm.nih.gov/34192700/)
61. R. Nieuwenhuys, L. Puelles, “The ‘wiring’ of the brain” in *Towards a New Neuromorphology* (Springer International Publishing, Cham, 2016), pp. 273–300.
62. I. Sarropoulos *et al.*, Developmental and evolutionary dynamics of cis-regulatory elements in mouse cerebellar cells. *Science* **373**, eabg4696 (2021). doi: [10.1126/science.abg4696](https://doi.org/10.1126/science.abg4696); pmid: [34446581](https://pubmed.ncbi.nlm.nih.gov/34446581/)
63. A. B. Butler, Evolution of the thalamus: A morphological and functional review. *Thalamus Relat. Syst.* **4**, 35–58 (2008). doi: [10.1017/S1472928808000356](https://doi.org/10.1017/S1472928808000356)
64. L. Puelles, Thoughts on the development, structure and evolution of the mammalian and avian telencephalic pallium. *Philos. Trans. R. Soc. Lond. B Biol. Sci.* **356**, 1583–1598 (2001). doi: [10.1098/rstb.2001.0973](https://doi.org/10.1098/rstb.2001.0973); pmid: [11604125](https://pubmed.ncbi.nlm.nih.gov/11604125/)
65. R. Heredia, Ma. Real, J. Suárez, S. Guirado, J. C. Dávila, A proposed homology between the reptilian dorsomedial thalamic nucleus and the mammalian paraventricular thalamic nucleus. *Brain Res. Bull.* **57**, 443–445 (2002). doi: [10.1016/S0361-9230\(01\)00712-2](https://doi.org/10.1016/S0361-9230(01)00712-2); pmid: [11923007](https://pubmed.ncbi.nlm.nih.gov/11923007/)
66. E. S. Lein *et al.*, Genome-wide atlas of gene expression in the adult mouse brain. *Nature* **445**, 168–176 (2007). doi: [10.1038/nature05453](https://doi.org/10.1038/nature05453); pmid: [17151600](https://pubmed.ncbi.nlm.nih.gov/17151600/)
67. D. Hain, Pogona scRNA-seq analysis, Max Planck Computing and Data Facility GitLab (2022); <https://doi.org/10.17617/1.91>.

Downloaded from https://www.science.org at University Van Amsterdam on April 13, 2025

SUPPLEMENTARY MATERIALS
science.org/doi/10.1126/science.abp8202
 Materials and Methods
 Figs. S1 to S20
 References (68–74)
 MDAR Reproducibility Checklist
 Data S1 to S8
 View/request a protocol for this paper from Bio-protocol.
 Submitted 28 February 2022; accepted 18 July 2022
 10.1126/science.abp8202